Proceedings of the 2016 International Conference on Wavelet Analysis and Pattern Recognition, Jeju, South Korea, 10-13 July

POINTER-TYPE METER AUTOMATIC READING FROM COMPLEX ENVIRONMENT BASED ON VISUAL SALIENCY

LIN ZHANG, BIN FANG, XING ZHAO, HONG-SUO ZHANG

College of Computer Science, Chongqing University, Chongqing, China
E-MAIL: lz@cqu.edu.cn, fb@cqu.edu.cn, xingzhao@cqu.edu.cn, fengqiusuo@cqu.edu.cn

Abstract:

This paper presents an automatic interpretation method for pointer-type meter reading from complex environment based on visual saliency. Compared with the manually based methods, the proposed approach is based on image processing and automatic technique, avoiding the problems of low efficiency, high subjective, as well as inaccurate precision that are caused by manual judgement. Firstly, a localized pixel inhomogeneity factor (LPIF) model is developed to improve the visual saliency of the pointer-type meter region. After binarization, the Hough circle detector is utilized to locate the approximate pointer region. In the candidate image region, the true pointer-type metre indicator is considered as the straight line with maximum length. Therefore, the Hough line transform is used to locate the precise pointer-type metre indicator. In the final step, the scale of metre-type meter reading is obtained by calculating the angle of pointer indicator. Experiments demonstrate that the proposed method is very effective on all kinds of pointer-type meter readings. And the proposed automatic scheme not only greatly economizes the labor cost, but also deals with life-threatening issues in dangerous environment.

Keywords:

Pointer-type meter reading; Automatic reading; Localized pixel inhomogeneity factor; Visual saliency; Image processing

1. Introduction

Nowadays, pointer-type meter has been widely used in test and control industries. Typical examples include pressure density meter, lightning arrester meter, oil level gauge, oil temperature gauge, and automobile instrument, *etc*. Pointer-type meter has many advantages, such as simple structure, low maintenance cost, strong resistance to electromagnetic interference, and high precision, *etc*. However, pointer-type meter generally has no cable interface. Hence, quite a large number of pointer-type meters data heavily depend on human observation. After a long labouring time, such manual work often lead to low efficiency, high subjectivity and unfair calibration bias that are caused by heavily physical exhaustion. Moreover, there are some dangerous occasions that cannot use human observation for pointer-type meter reading. Thus, it is of great significance to develop an automatic reading scheme for pointer-type meter.

Over the past few years, many academic papers that involve pointer-type meter have been published. In [1], Liu *et al.* fitted a straight line using the least squares fitting method. This method has a good fault tolerance and robustness in images with simple background. Shi *et al.* [2] proposed a pointer-type meter detection method to remotely detect meter reading data. This method is very suitable for images with uniform illumination. Based on the traditional Hough transform, Han *et al.* [3] proposed an improved scheme to extract pointer indicator. Besides, Yue *et al.* [4] introduced an automatic Hough transform to read the meter numbers. In addition, Sun *et al.* [5] proposed an improved pointer angle recognition algorithm named the concentric ring search method with much higher detection accuracy. Based on binocular vision, Biao *et al.* [6] integrated fast Hough transform and three-dimensional space reconstruction to read the pointer indicator. According to their paper, their method has a higher reading precision. Guan *et al.* [7] observed that pointer was obvious than the sounding region. Thus, they combined image difference with calibration mapping for the detection. All of the aforementioned methods aim to recognize pointer-type meter in simple background. And these methods will fail in complex environment.

In this paper, an automatic pointer-type meter reading method is proposed to recognize the pointer in complex environment based on visual saliency. There are two contributions. 1) Firstly, a localized pixel inhomogeneity factor (LPIF) model is proposed for image binarization. 2) Secondly, a general reading procedure is particularly designed for all kinds of pointer

978-1-5090-2917-4/16/$31.00 ©2016 IEEE

meter. Figure 1 displays the block diagram of the proposed method for pointer-type meter automatic reading.

FIGURE 1. Flowchart of the proposed automatic reading scheme.

2. Methodology

2.1. Image preprocessing

Typically, the pointer-type meters may differ according to their installed occasions. Figure 2 shows some of the examples that are captured by our cameras. In viewing of this figure, the proposed method should be well designed to meet the specification of different kinds of point-type meters. As listed in Figure 2, the complex occasions include: 1) dark background; 2) highlight background; 3)complicated environment; 4) pointer-type-meter-like objects.

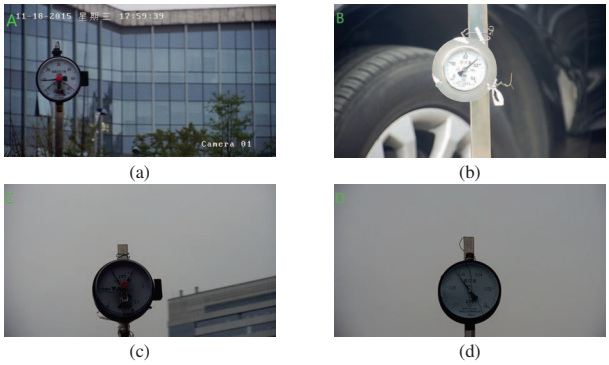

FIGURE 2. Examples of the pointer-type meter images.

Inspired by the visual mechanism of human-beings, the saliency detection literature attends to only salient location in the image [8]. And in the theory of *Inhomogeneity Neighborhood Propagation* (INP), pixels in one target texture do not simply adhere to piecewise-constant or piecewise-smooth homogeneity in brightness [9]. Thus, INP works in a bottom-up manner. It repeatedly aggregates the inhomogeneous neighbors together using a *Pixel Inhomogeneity Factor* (PIF) decision rule. In this manner, these steps form many independent saliently textured regions that are constituted with adjacent inhomogeneous pixels. In [10], the authors used the idea of PIF for object segmentation in nature scenario. Note that in our pointer-type meter images, each image contains only one meter indicator. By using the PIF decision rule, the foreground of pointer-type meter is highlighted.

Benefits of PIF decision rule come from the following aspects: 1) Part of the metre region may be seriously polluted by dust. The global threshold based methods disregard the connectivity of a meter object. 2) INP considers the variance of local neighboring pixels. It is an anti-polluted method and also well appropriate for our problem.

Given a gray-level image I, p is a pixel in image I. Denoted by $L(p)$ the spatial neighborhoods of p, there are few pixels in $L(p)$ that have the same intensity of p. To visually demonstrate the results of intermediate experiments, we take the gray-level of Figure (A) as input. From Figure 2, one can observe that the intensity of pointer-type meter region clearly differs with its background. Thus, the salient calculation can be used to distinguish them. Define two pixels set as follows:

$$\Omega_1 = \{q \in L(p) : |I(p) - I(q)| < t\} \tag{1}$$

$$\Omega_2 = \{q \in L(p) : |I(p) - I(q)| > t\} \tag{2}$$

where p and q are two pixels of I, and $L(*)$ represents the neighborhoods of p or q. The threshold t is calculated as:

$$t = \frac{\sum_{p \in L(p), q \in L(p), q \neq q} |I(p) - I(q)|}{N} \tag{3}$$

where N is the number of pixels in image I.

The pixels in Ω_1 are similar with p, while the pixels in Ω_2 are dissimilar with p. If we fix the size of $L(p)$, there will be more pixels in Ω_1 but less in Ω_2. These two parts are complementary.

Define the PIF of a single pixel as:

$$\text{PIF}(p) = \frac{|\Omega_2|}{|L(p)|} \tag{4}$$

PIF is considered as the brightness difference between a center pixel and its neighborhoods. When there is great variance of intensity around square neighborhood, PIF will become big. In this case, they belong to inconsistent area. For example, the ultimate pixels host at both the target resident and the background edge.

In PIF, t is a global threshold for image I. As a result, PIF still has some defects, as the global binarization technique does. Moreover, if there contains certain noise around p, the result may be much worse. In order to solve these issues in global PIF, we propose a *Localized Pixel Inhomogeneity Factor* (LPIF) computational model. LPIF utilizes PIF in local patches. The difference is that LPIF weights the pixels using

Gaussian weights. In general, the main procedure of LPIF can be summarized as follows:

(a) Let p be the center pixel. In the beginning, $i \leftarrow 0$, $S_0(x,y) \leftarrow p$, $I_0(x,y) \leftarrow p$, then $I_0(x,y)$ contains only 1 pixel. Now let $i \leftarrow i+1$ and go to next step.

(b) $S_1(x,y)$ contains all the neighborhoods of $S_0(x,y)$ within 1 pixel distance. Let $i \leftarrow 1$ and update I_1 by $I_1(x,y) = S_0(x,y) \bigcup S_1(x,y)$. Obviously, $I_1(x,y)$ contains 3×3 pixels.

(c) Similarly, $S_2(x,y)$ are the neighborhoods of $S_1(x,y)$ with 1 pixel in spatial distance. Note that $S_2(x,y)$ does not include the pixels in $I_1(x,y)$. Let $i \leftarrow 2$, then $I_2(x,y) = S_0(x,y) \bigcup S_1(x,y) \bigcup S_2(x,y)$. Now $I_2(x,y)$ contains 5×5 pixels.

(d) Suppose that $S_n(x,y)$ contains the neighborhoods of $S_{(n-1)}(x,y)$ within 1 pixel but not the elements in $I_{(n-1)}(x,y)$. Let $i = n$. Update $I_n(x,y)$ by $I_n(x,y) = S_0(x,y) \bigcup S_1(x,y) \bigcup S_2(x,y) \bigcup \cdots \bigcup S_n(x,y)$. It is easy to see that $I_n(x,y)$ totally contains $(2n+1) \times (2n+1)$ pixels.

From above analyses, one can derive the equation of $I_i(x,y)$

$$I_i(x,y) = S_0(x,y) \bigcup S_1(x,y) \bigcup S_2(x,y) \bigcup \cdots \bigcup S_n(x,y) \tag{5}$$

For simplicity, (5) can be rewritten in a shortened form:

$$I_i = S_0 \bigcup S_1 \bigcup S_2 \bigcup \cdots \bigcup S_n \tag{6}$$

Salience can be expressed as:

$$S_i(x,y) - \text{means}(S_{(i-1)}(x,y)) \tag{7}$$

The connection between 7 and LPIF(x,y) is shown as:

$$\text{LPIF}(x,y) = \begin{cases} 1, & \text{if } S_i(x,y) - \text{means}(S_{(i-1)}(x,y)) > 0 \\ 0, & \text{if } S_i(x,y) - \text{means}(S_{(i-1)}(x,y)) \leq 0 \end{cases} \tag{8}$$

where means$(S_i(x,y))$ is calculated by:

$$\text{means}_i = \iint_{\Omega} K_G(x,y) I_i(x,y) dxdy \tag{9}$$

The Gaussian weighted average makes the salience evidently. In our problem, $K_G(x,y)$ is a two-dimensional Gaussian weighting. The $K_G(x,y)$ function is defined by:

$$K_G(x,y) = ae^{\frac{-(x^2+y^2)}{2\sigma^2}} \tag{10}$$

where σ is the radius of convolution kernel, a is a normalized parameter.

Based on the definitions above, the LPIF function is expressed by:

$$\text{LPIF}(p) = \frac{\sum_{i=1}^{n} \text{LPIF}}{n} \tag{11}$$

In the paper of [11], the threshold is obtained in iteration. The authors in [12] introduced a local patch based threshold technique to remove non-homogeneous background. However, these routines are not suitable for the occasion in Figure 2. The image of Figure 2 (A) can be divided into multiple square regions. If we use a hard threshold, some useful information may be lost.

In Figure 3, we compare the visual results that are obtained by global binarization, PIF, and the proposed LPIF technique.

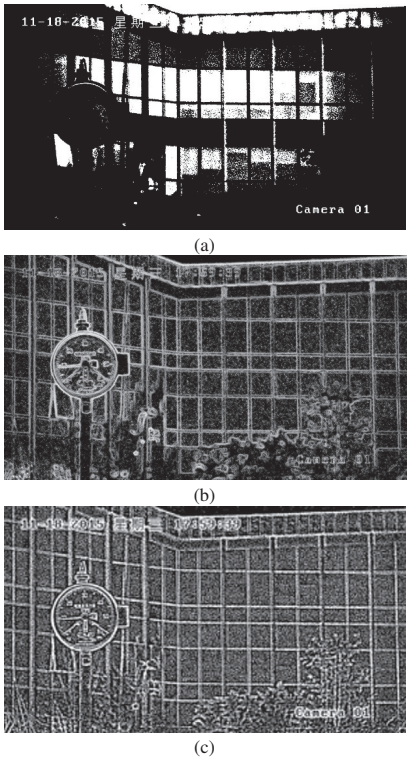

(a) (b) (c)

FIGURE 3. (a) Global binary image and, (b) PIF result image, (c) LPIF result image.

We summarize the advantages of the proposed LPIF as following: 1) This method is a localized method. Thus, it avoids the drawbacks of the global threshold based methods. 2) This method is noise-resistance. 3) Benefiting from the simulation of visual mechanism, the target object is much clearer when filtered with LPIF.

2.2. Round Dial Location

Many of the research papers pointed out that by setting some parameters, such as minimum/maximum radius, the Hough circle detector works well to locate the centre of a circle along with the corresponding radius. The Hough circle detector converts the binary image space into a parameter space. The global characteristics are fully utilized to find out the best votes for the predefined parameters. The most inspiring property of Hough transform is that it can give robust detection under noise and partial occlusion. Here, we simply use the Matlab built-in function "*imfindcircles*" to find out the region of round dial by passing the mininum/maximum radius as input parameters. The extracted circular dial is shown in Figure 4:

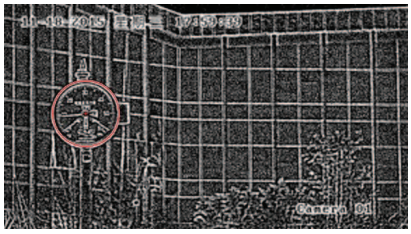

FIGURE 4. Detected round dial region (marked in red circle).

The drawn red circle shows that the precision of Hough circle detection is high. The result after background removal is shown in Figure 5.

FIGURE 5. Round target binary image.

2.3. Pointer Detection

Pointer-type meter indicator detection plays an important role in the proposed algorithm. Moreover, an inconspicuous bias may lead to inaccurate reading. In our image data set, pointer is the longest line that can be detected using Hough transform. The theory behind Hough transform is the duality between line and point. On the one hand, the collinear points in image space correspond to the non-collinear lines in parameter space. On the other hand, all lines which intersect at a same point in the parameter space, correspond to a point of non-collinear lines in image space. Therefore, Hough transform converts a line detection problem in image space into a point detection problem in parameter space. Detection task is achieved by making a statistical analysis in the parameter space.

If line equation is adopted in parameter space, and if the slope of this line is infinity in parameter space, the accumulator changes sharply, leading to expensive computational bottleneck. To deal with this issue, Hough line detector uses the following function:

$$\rho = x\cos(\theta) + y\sin(\theta) \tag{12}$$

where (x, y) denotes the image space, while (ρ, θ) indicates the parameter space.

According to this equation, the point in the image space corresponds to a sine curve in the parameter space. The detection is described as follows: Let θ be an given positive floating number, then calculate ρ by the fixed θ. This leads to an accumulated array of θ and ρ. And then we obtain the number of collinear points. Figure 6 displays an example where the pointer indicator locates in the first quadrant:

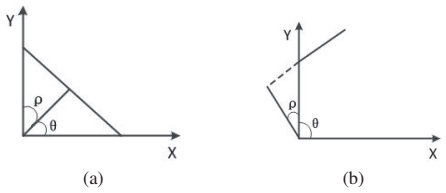

FIGURE 6. Straight line position in the first quadrant image.

Where the range of θ is $[0°, 180°]$. The obtained pointer is shown in Figure 7 with cyan solid line overlaid on the original color image.

FIGURE 7. Pointer detection result image.

2.4. Scale Calculation

Yang *et al.* [6] stated that there are mainly two approaches that have been used in interpretation of the meter from its input image. The first one is to detect the pointer indicator and the scale that it points to. This approach had also been used in [13] and [14]. The other one is to calculate the angle between the pointer indicator and the zero position. Specifically, the first approach directed recognizes the number of the pointer, while the second method infers the reading number according to the correspondence between the pointer position and the calculated scale. In this paper, we adopt the latter method for calculation.

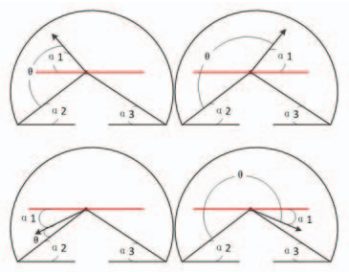

FIGURE 8. Four situations to compute θ image.

One can see that there is a distinct feature in all pointer-type meters: The angle between the horizontal line and the zero/maximum position is constant and invariant. Let α_2 mark the angle between the zero position and the horizontal line, and α_3 mark the angle between the maximum position and the horizontal line, respectively. Figure 8 depicts the two concepts. Both α_2 and α_3 are obtained by priori knowledge. Assume that α_1 is the angle between pointer indicator and the horizontal line, and θ is the angle from zero position to pointer indicator. According to the cases shown in Figure 8, the equations of θ are calculated accordingly. We summarize them in Table 1.

TABLE 1. Computational formulation of θ.

#case	α_1	θ
1	-	$\theta = \alpha_2 - \alpha_1$
2	+	$\theta = \alpha_2 + \pi - \alpha_1$
3	+	$\theta = \alpha_2 - \alpha_1$
4	-	$\theta = \alpha_2 + \pi - \alpha_1$

Assume that x is the reading number, and len is the range of the round dial. Then, we count the reading indication of the meter by the following equation:

$$\frac{\theta}{pi + \alpha_2 + \alpha_3} = \frac{x}{len} \tag{13}$$

3. Experimental Results

FIGURE 9. Periodic result of different original input image.(The four columns respectively displays the results of LPIF filtering, meter dial detection, the PIF detected pointer lines, and the LPIF detected pointer lines using the meter images listed in Figure 2.)

This section we will show some results of the proposed method. In Figure 9, the last two column represent the PIF detected lines and the LPIF detected lines, respectively. Because LPIF is localized and noise-resistant, so both the circles (the second column) and the lines (the fourth column) are detected accurately. One main feature of pointer-type meter images is characterized by the image intensity. Other factors, such as the nameplates, may degrade the quality of binary images and lead to a wrong reading result. While LPIF makes the object clear to be recognized according to the visual saliency, and insure accurate detection of circles and lines, which demonstrate the advantage of the proposed method using LPIF.

For quantitative comparison, Table 2 shows the reading results of the seven test images using the PIF method and the proposed LPIF method. Seven pointer meter images (numbered as "A", "B", $\cdots$, "G") have been used for experiment. Specifically, "A" is blurry, "B" is with a strong light on it, "C" is contrary to "B", taking a dark light, and "D" has a crack on the surface of meter dial (which are shown in Figure 2). The "value" column in Table 2 represents the manual reading of pointer indicator. If i=1, there used PIF method; and if i=2, there used proposed LPIF method,and the "error(i)" in Table 2

is calculated by the following equation.

$$\text{error(i)} = \frac{|value - result(i)|}{|value|} \tag{14}$$

Quantitative results show that the proposed method works well under these challenging conditions (complex environment, disturbing noises, and light effection). Besides, from Table 2, we can observe that the reading results of the proposed method are more accurate than the PIF method.

TABLE 2. Calculated results of detected pointer meter.

#	center	radius	value	result1	result2	error1(%)	error2(%)
A	(193,264)	78.65	9	8.7310	9.0536	2.99	0.06
B	(461,231)	85.02	0.26	0.2715	0.2711	4.26	3.03
C	(421,371)	109.16	1	0.9786	0.9802	2.14	1.98
D	(478,378)	109.02	-0.064	-0.0635	-0.0637	0.78	0.47
E	(500,417)	88.77	0.32	0.3272	0.3255	2.25	1.71
F	(500,367)	77.56	0.26	0.2676	0.2674	2.92	2.84
G	(511,387)	98.50	22	20.4672	21.7224	6.96	1.26

4. Conclusions

This paper proposes a method of reading pointer-type meter automatically. Through the improved LPIF model, the proposed method settles the problems of complicated background and unequal illumination. The Hough circle detector is used to locate the approximate region of the pointer dial, then the Hough line detector is utilized to find out the pointer indicator. And at the final step, we calculate the reading numbers from the point scale. The experimental results validate that the proposed algorithm is adequate for the reading of pointer-type meter in terms of accuracies. In the future, we can use the multi-scale analysis method to improve the speed and efficiency.

Acknowledgements

This paper is supported by National Natural Science Foundation of China (61472053, 91420102), China Postdoctoral Science Foundation (2014M550456), Chongqing Postdoctoral Special Funding Project (Xm2014087), and Chongqing University Postgraduates' Innovation Project (No. CYS15019).

References

[1] S.-G. Liu, M.-Y. Liu, and Y. He. Checking on the quality of gauge panel based on wavelet analysis. In *Machine Learning and Cybernetics, 2002. Proceedings. 2002 International Conference on*, volume 2, pages 763–767 vol.2, 2002.

[2] Z. Shi, K. HE, Y. J.K., and M. Design of remote meter reading method for pointer type chemical instruments. *Process Automation Instrumentation*, 2014.

[3] H. Jiale, L. En, T. Bingjie, and L. Ming. Reading recognition method of analog measuring instruments based on improved hough transform. In *Electronic Measurement Instruments (ICEMI), 2011 10th International Conference on*, volume 3, pages 337–340, Aug 2011.

[4] X. feng Yue, Z. Min, X. dong Zhou, and P. kai Wang. The research on auto-recognition method for analogy measuring instruments. In *Computer, Mechatronics, Control and Electronic Engineering (CMCE), 2010 International Conference on*, volume 2, pages 207–210, Aug 2010.

[5] F.-j. Sun, F.-s. Guo, J.-q. Fan, and T.-b. Wang. Studies of the recognition of pointer angle of dial based on image processing. *PROCEEDINGS-CHINESE SOCIETY OF ELECTRICAL ENGINEERING*, 25(16):73, 2005.

[6] B. Yang, G. Lin, and W. Zhang. Auto-recognition method for pointer-type meter based on binocular vision. *Journal of Computers*, 9(4):787–793, 2014.

[7] G. Yudong, Z. Yang, H. Bowen, Z. Hong, and S. Dayu. Pointer-type meter reading method research based on image processing technology. In *Networks Security Wireless Communications and Trusted Computing (NSWCTC), 2010 Second International Conference on*, volume 1, pages 107–110. IEEE, 2010.

[8] X. Hou and L. Zhang. Saliency detection: A spectral residual approach. In *Computer Vision and Pattern Recognition, 2007. CVPR '07. IEEE Conference on*, pages 1–8, June 2007.

[9] J. Ding, J. Shen, H. Pang, S. Chen, and J. Yang. Exploiting intensity inhomogeneity to extract textured objects from natural scenes. In *Computer Vision–ACCV 2009*, pages 1–10. Springer, 2009.

[10] J. Ding, R. Ma, and S. Chen. A scale-based connected coherence tree algorithm for image segmentation. *IEEE Transactions on Image Processing*, 17(2):204–216, Feb 2008.

[11] X. Ye, D. Xie, and S. Tao. Automatic value identification of pointer-type pressure gauge based on machine vision. *Journal of Computers*, 8(5), 2013.

[12] Y. Wang, B. Fang, L. J. Lan, H. W. Luo, and Y. Y. Tang. Adaptive binarization: A new approach to license plate characters segmentation. In *Wavelet Analysis and Pattern Recognition (ICWAPR), 2012 International Conference on*, pages 91–99, July 2012.

[13] Y. Y. Z. Y. H. Xiaoyan and T. Pei. Automatic calibration of analog measuring instruments using computer vision. *Chinese Journal of Scientific Instrument*, page S1, 2001.

[14] L.-s. ZHANG, C.-h. SUI, and J.-p. TONG. Automatic recognition of analog pointer meter based on image processing method. *Journal of Zhejiang University of Technology*, 3:001, 2008.